Elastic Scattering of Alpha Particles by C^{12} in the Bombarding Energy Range 10 to 19 MeV*

E. B. CARTER,† G. E. MITCHELL,‡ AND R. H. DAVIS
Department of Physics, Florida State University, Tallahassee, Florida
(Received 7 October 1963)

The scattering of alpha particles by C^{12} has been studied in the bombarding energy range 10 to 19 MeV. Many anomalies were observed in the excitation curves which correspond to O^{16} compound system energy levels in the excitation energy range 14 to 21 MeV. Fifteen detailed angular distributions were measured and the data have been analyzed with a smooth cutoff model which was modified to include appropriate resonant phase shifts. The spins and parities of the more prominent resonances have been assigned. Real well depths of 100 MeV or more were required in an optical-model analysis to yield theoretical cross sections comparable with experimental values. In general, optical-model fits were not satisfactory. Two series of levels in O^{16} were observed which obey rotational band systematics. The substantial widths of the band members suggest an alpha-particle cluster configuration for these excited states.

I. INTRODUCTION

THE bombarding energy range of the alpha-particle beam produced by the Florida State University tandem Van de Graaff accelerator is approximately 6 to 19 MeV. This beam was used to study the excited states of O^{16} in the excitation energy range 14 to 21 MeV by observing the elastic scattering of alpha particles from C^{12}. A concurrent inelastic scattering experiment is discussed in the following paper.[1]

The elastic scattering of alpha particles by C^{12} has been experimentally studied and the data interpreted with compound nucleus analysis by Hill[2] (bombarding energy up to 3 MeV), Bittner and Moffat[3] (3 to 7 MeV), and by Ferguson and McCallum[4] (7 to 11 MeV). At higher energies, 17 to 48 MeV, cyclotron alpha-particle beams[5–7] have been used to study the scattering of alpha particles by carbon. Igo and Thaler[8] have fitted data at 40.2 MeV with the nuclear optical model. An analysis of cyclotron data based on exchange scattering has been given by Honda *et al.*[9]

Data obtained in a number of alpha-particle scattering experiments with targets heavier than carbon have been fitted with the nuclear optical model[8,10,11] and with the cutoff or diffraction model.[12–14] Both of these models are applied in this paper. The sharp cutoff model is denoted herein by APB for the contributions of Ackhiezer and Pomeranchuk[12] and of Blair.[13] A smooth absorption dependence on l was introduced by McIntyre *et al.*[15] and by Ellis and Schecter,[16] and the modified model is referred to here as the APBM model.

Above 10 MeV, two or more channels are open and resonances are seldom well isolated, but the optical-model assumption of dense, overlapping levels is not satisfied by the data. Only limited success in the application of the optical model was anticipated. Real well depths in excess of 100 MeV were required for even crude fits to the data.

Spins and parities of the more prominent resonances were tentatively assigned from the behavior of the excitation curves at selected angles. Confirmation was obtained from the analysis of the angular distributions with a smooth cutoff model modified to include resonances. Resonant phase shifts indicated by the tentative assignments were adjusted to best fit the angular distributions. Other phase shifts computed with the cutoff models are slowly varying with energy and were used as effective "hard-core phase shifts" in the analysis of resonances.

While the compound system O^{16} is a doubly closed shell nucleus, the application of the shell model to the states observed in the present experiment is complicated by the high excitation energy. The ground state and low-lying excited states have been extensively discussed, and the scope of the model has been enlarged to

* Supported in part by the U. S. Air Force Office of Scientific Research.
† Present address: Rice University, Houston, Texas.
‡ Present address: Columbia University, New York, New York.
[1] G. E. Mitchell, E. B. Carter, and R. H. Davis, Phys. Rev. **133**, B1434 (1964), following paper.
[2] R. W. Hill, Phys. Rev. **90**, 845 (1953).
[3] J. W. Bittner and R. D. Moffat, Phys. Rev. **96**, 374 (1954).
[4] A. J. Ferguson and G. J. McCallum, Bull. Am. Phys. Soc. **6**, 235 (1961); and private communication.
[5] G. Igo, H. E. Wegner, and R. M. Eisberg, Phys. Rev. **101**, 1508 (1956); A. I. Yavin and G. W. Farwell, Nucl. Phys. **12**, 1 (1959). C. Hu. S. Kato, Y. Oda, and M. Takeda, J. Phys. Soc. Japan **14**, 1184 (1959); J. Aguilar, W. E. Burcham, J. Catala, J. B. A. England, J. S. C. McKee, and J. Rotblat, Proc. Roy. Soc. (London) **A254**, 395(1960); V. K. Rasmussen, D. W. Miller, and M. B. Sampson, Phys. Rev. **100**, 181 (1955); J. D. Jodogne, P. C. Macq, and J. Steyaert, Phys. Letters **2**, 325 (1962); R. A. Atneosen, H. L. Wilson, M. B. Sampson, and D. W. Miller, Bull. Am. Phys. Soc. **8**, 303 (1963); H. F. Lutz, J. B. Mason, and C. T. Paulson, Nucl. Phys. **43**, 405 (1963); G. Igo and B. D. Wilkins, Phys. Rev. **131**, 1251 (1963).
[6] J. C. Corelli, E. Bleuler, and D. J. Tendam, Phys. Rev. **116**, 1184 (1959).
[7] Takashi Mikumo, J. Phys. Soc. Japan **16**, 1066 (1961).
[8] G. Igo and R. M. Thaler, Phys. Rev. **106**, 126 (1957).
[9] T. Honda, Y. Kudo, and H. Ui, Nucl. Phys. **44**, 472 (1963).
[10] R. M. Eisberg and C. E. Porter, Rev. Mod. Phys. **33**, 190 (1961).
[11] G. Igo, Phys. Rev. **115**, 1665 (1959).
[12] A. Ackhiezer and I. Pomeranchuk, J. Phys. (U.S.S.R.) **9**, 471 (1945).
[13] J. S. Blair, Phys. Rev. **95**, 1218 (1954).
[14] D. D. Kerlee, J. M. Blair, and G. W. Farwell, Phys. Rev. **107**, 1343 (1957).
[15] J. A. McIntyre, K. H. Wong, and L. C. Becker, Phys. Rev. **117**, 1337 (1960).
[16] R. E. Ellis and L. Schecter, Phys. Rev. **101**, 636 (1956).

include collective excitation modes.[17] The alpha-particle model of Dennison,[18] which was extended by Kameny[19] has been surprisingly successful. A number of alpha-particle widths have been qualitatively explained in terms of the cluster model by Roth and Wildermuth.[20]

Level parameters have been assigned to most of the prominent resonances. From an examination of the energies and spins, two rotational bands of levels were identified and two additional bands are tentatively suggested. The appropriate cluster model wave functions are labeled.

II. EXPERIMENTAL TECHNIQUES

Alpha-Particle Beam

Negative helium ion injection into a tandem Van de Graaff accelerator to produce 19-MeV alpha-particle beams has been discussed by Carter and Davis.[21] It is sufficient to mention just a few pertinent facts here. Helium gas is fed into the duo-plasmatron ion source provided with the accelerator. Hydrogen is used in the electron pickup canal and is much more effective than air or helium. The momentum of the negative ion beam injected into the Tandem corresponds to that of a He^+ ion coming from the duo-plasmatron ion source and a He^- ion coming from the electron pickup canal. The ion source electrical parameters (arc current, arc voltage, and filament current) are similar to those for other ions. Focusing is rather critical and both of the einzel (unipotential) lenses between the ion source analyzing magnet and the accelerator were used. Beam currents were normally 5 to 20 mμA.

Scattering Experiment

Alpha particles were scattered by thin carbon foil targets mounted in a target chamber specifically designed for solid-state counter utilization.[22] The self-supporting targets were films of colloidal graphite[23] which were 25 to 100 $\mu g/cm^2$ thick.

Because of the low counting rates, simultaneous use of several particle counters was advantageous. As many as eight excitation curves were measured at the same time. Three detectors were used for the angular distribution measurements. Pulse-height distributions of three to eight counters were measured and displayed by one or two TMC 265-channel analyzers with suitable memory splitting.

Due to some initial difficulty in focusing the beam through small collimators, large beam defining slits and detectors were necessary. The often sharp dependence of the elastic scattering cross section on the angle made angular uncertainty the most important error. The angular uncertainty was reduced as its importance became evident and as the available beam current increased.

Errors in angle due to (1) angular resolution and (2) angular reference were considered. The first is a result of finite beam spot and detector size, and limits the angular range within which scattered particles were counted. The second is primarily a function of beam position on target and the beam axis location within the collimation limits. The angular resolution and angular error limits in the laboratory system are, respectively: ± 3.3 and $\pm 2.0°$ lab for the excitation curves labeled 109.5, 140.8, and 159.7 deg c.m.; ± 4.4 and $\pm 2.9°$ lab for the 70.4, 90.0, and 125.2 deg c.m. curves; ± 1.0 and $\pm 0.8°$ lab for the remaining set of eight excitation curves; and ± 2.3 and $\pm 1.6°$ for the angular distributions.

The errors due to accelerator energy spread and beam energy loss within the target are included in the resultant energy resolution tabulated in Table I. The

TABLE I. Energy resolution and cross-section error.

Bombarding energy	Energy resolution, including target thickness and beam energy resolution in keV 10 MeV	19 MeV	Absolute cross-section error (rms)
70.4°, 125.2°, 159.7° c.m. excitation curves (Fig. 1)	63	53	±18%
90°, 109.5°, 140.8° c.m. excitation curves (Fig. 1)	176	114	±18%
8 excitation curves (Figs. 2 and 3)	40	44	±11%
Angular distributions	100	72	±13%

beam energy analyzing magnet was calibrated by a measurement of the $C^{13}(p,n)N^{13}$ reaction threshold assuming a value of 3.2372 ± 0.0016 MeV. Magnet linearity up to 17.5-MeV protons or He^{++} was confirmed by performing $Li^7(\alpha,n)B^{10}$ reaction threshold measurements with both He^+ and He^{++} beams.

Cross sections were determined by normalization of the data to the results of previous experiments. Because of hydrogen and oxygen contaminants and possible surface roughness, it was difficult to measure the target thickness directly.

Normalizations to the $C^{12}(\alpha,\alpha)C^{12}$ data of Bittner and Moffat[3] and to that of Ferguson and McCallum[4] agreed within 2%, well within the estimated experimental error of 6%. The angular distributions were normalized to the excitation curves which overlapped the previous measurements. The remaining excitation

[17] J. J. Griffin, Phys. Rev. **108**, 328 (1957).
[18] D. M. Dennison, Phys. Rev. **96**, 378 (1954).
[19] G. L. Kameny, Phys. Rev. **103**, 358 (1956).
[20] B. Roth and K. Wildermuth, Nucl. Phys. **20**, 10 (1960).
[21] E. B. Carter and R. H. Davis, Rev. Sci. Instr. **34**, 93 (1963).
[22] P. B. Weiss, Ph.D. dissertation, Florida State University, 1963 (to be published).
[23] "Dag" Solution No. 154, Acheson Colloids, Port Huron, Michigan (unpublished).

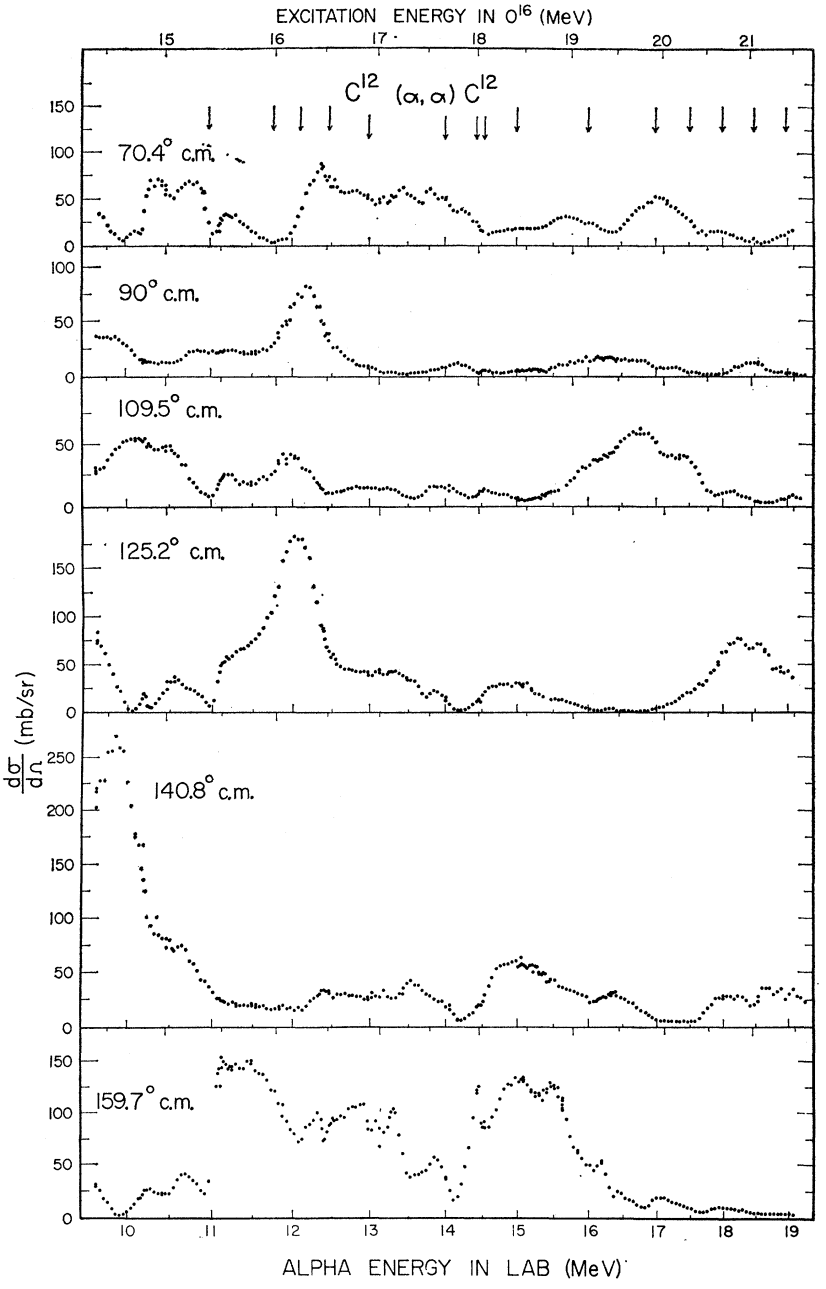

FIG. 1. Six excitation curves of $C^{12}(\alpha,\alpha)C^{12}$. The arrows indicate the energies at which detailed angular distributions were measured.

curves were then normalized to the angular distributions. Yields from the separate detectors used within each angular distribution were normalized to make smooth curves for both the elastic and inelastic angular distributions. The estimated cross section errors are tabulated in Table I.

III. RESULTS

Excitation Curves

The fourteen elastic scattering curves (Figs. 1–3) show large resonant structure despite the high excitation energy (14 to 21 MeV in the O^{16} compound system). The structure does not close up into a continuum as the energy is increased over this energy span. In this energy region, the $C^{12}(\alpha,\alpha_1)C^{12*}$ excitation curves show relatively less structure.[1] Fewer resonances appear in the $C^{12}(\alpha,p_0)N^{15}$ excitation curves (Fig. 4) or the $C^{12}(\alpha,n)O^{15}$ excitation curves[24] than in the $C^{12}(\alpha,\alpha)C^{12}$ data.

Several prominent anomalies appear in the elastic excitation curves at bombarding energies of 9.9, 11.3,

[24] R. D. Carpenter, L. R. Mentillo, and E. Bleuler, Phys. Rev. **125**, 282 (1962); J. W. Nelson, E. B. Carter, G. E. Mitchell, and R. H. Davis, Phys. Rev. **129**, 1723 (1963).

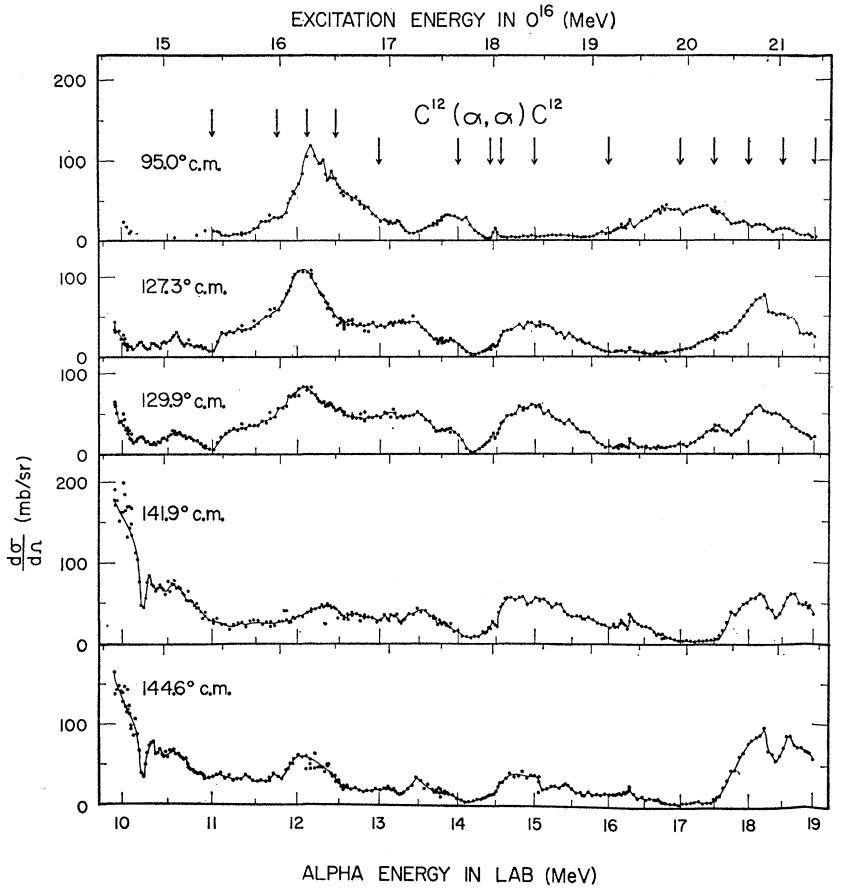

FIG. 2. Five excitation curves of $C^{12}(\alpha,\alpha)C^{12}$. The arrows indicate the energies at which detailed angular distributions were measured.

12.1, 13.0, 15.1, and 18.5 MeV. In addition there are some 20 lesser anomalies with observed widths from 40 to 500 keV. The possible angular errors were taken into account in assigning the levels listed in Table II and in drawing the solid experimental lines in the figures.

The $C^{12}(\alpha,p_0)N^{15}$ cross section (Fig. 4) is much smaller then the $C^{12}(\alpha,\alpha)$ or $C^{12}(\alpha,\alpha_1)$ cross sections. Resonances are seen at 10.35-, 11.10-, 12.4-, 14.0-, and 14.75-MeV bombarding energy. A possible very broad level, ~1300 keV, is centered at 12.6 MeV. Because of high background and low yield a probable error of 0.3 mb/sr is assigned to each point in the (α,p_0) curves.

Angular Distributions

The angular distributions in Fig. 8 show the effects of the resonant structure apparent in the excitation curves. The prominent resonances at 12.1 and 18 MeV cause more maxima and minima to appear in the angular distributions, and the sharp resonance at 14.42 MeV is manifest in the difference between angular distributions observed at 14.42 and 14.53 MeV.

An unusual change in angular distribution character takes place from 18 to 19 MeV. The behavior of the angular distributions at extreme backward angles suggest a maximum at 180° for most energies and possibly all energies. Wong and Bleuler[25] have extended the 18.7-MeV angular distribution back to 179°. They find that the cross section at 180° is about 1.2 b/sr. This may be ascribed to some exchange process.[9] However, as far back as 165° the excitation curves show pronounced resonance effects. Large anomalies have been observed at 176° c.m. by Jodogne *et al.*[5] in the bombarding energy range 15 to 22.7 MeV.

The $C^{12}(\alpha,\alpha)C^{12}$ angular distribution at 18.0 MeV of Corelli, Bleuler, and Tendam[6] was substantially confirmed. A slight difference in shape of the angular distribution and the fact that our average cross section is about 25% higher may be explained by a difference in energy of 150 to 200 keV, which is within their quoted experimental error (1% in beam energy).

IV. ANALYSIS

Orientation

The cross section fluctuated rapidly with energy; there are a large number of resonances, often overlapping. Since the cross-section contour as a function of angle and energy was not measured in sufficient detail to promise a unique determination of all the phase

[25] S. S. M. Wong and E. Bleuler, Phys. Rev. **125**, 208 (1962).

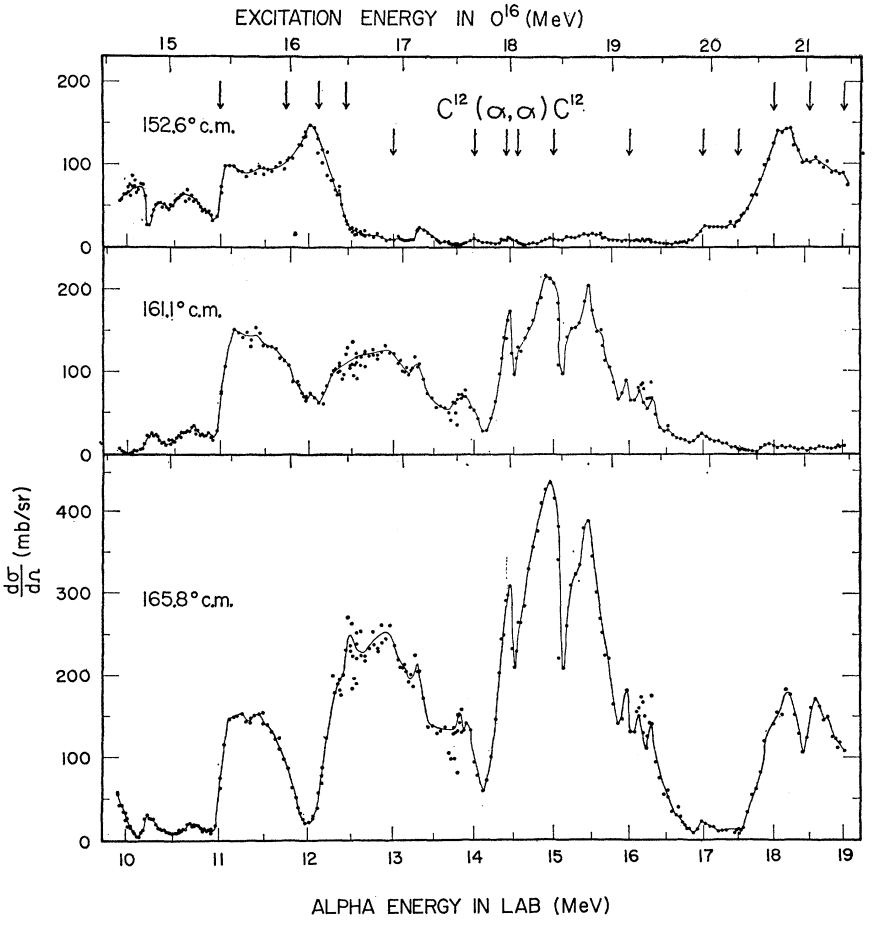

FIG. 3. Three excitation curves of $C^{12}(\alpha,\alpha)C^{12}$. The arrows indicate the energies at which detailed angular distributions were measured.

shifts, attempts were made to fit the data with the optical model, the Ackhiezer-Pomeranchuk–Blair (APB) sharp cutoff model[12,13] and the Ackhiezer-Pomeranchuk-Blair-McIntyre (APBM) smooth cutoff model.[15,16] In these models, there is no mechanism which can yield the anomalies observed in the excitation curves. To fit angular distribution data with the APBM model at or near anomalies, resonant phase shifts were added. In terms of phase-shift analysis, the model was used to compute the hard-sphere phase shifts and the phase-shift contributions of other resonances.

Preliminary spin and parity assignments to prominent

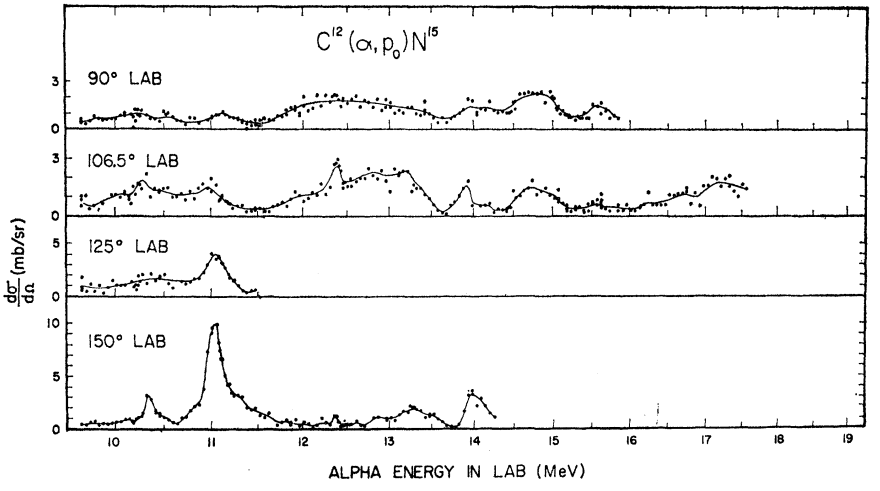

FIG. 4. $C^{12}(\alpha,p_0)N^{15}$ excitation curves. The statistical error on each point is about 0.3 mb/sr because of high background.

TABLE II. Energy levels in O^{16}.

This work					Previous work			
E_α (MeV)	E_x (MeV)	J^π	Γ (MeV)	Decay	E_x (MeV)	J^π	Γ (keV)	Decay
					13.97	2^-	22	p_0,α_1
					(14.2)	(2^+)		α_0,γ
9.9	14.6	even	450	α_0	14.72	2^+	300 to 1500	$p,\alpha_1,\alpha_0,\gamma$
10.18	14.78	$(0^+,1^-)$	60	α_0	14.81	0^+	40	α_0,α_1
10.25	14.85		75	p_0,α_0	14.92	4^+(odd l_p)	43	p_0,α_0,α_1
					15.21	2^-	72	p_0,α_1
					15.25	2^+	720	α_1,p_0
11.03	15.41	$(1^-,3^-)$	60	α_0,p_0	15.39	$1^-,2^+,3^-,4^+$	100	p_0,α_1
(11.08)	(15.45)		380	p_0,α_0	(15.43)		200	α_0,α_1
11.4	15.7	3^-	525	α_0	15.8		399 to 400	α_1,α_0,p_0
					(15.85)	(2^+)	~25	n,γ
					15.95			p_α,α_0
					16.06	(2^+)	~50	n,α_1,p_0,γ
12.1	16.2	6^+	380	α_0	16.2	$4^+,5^+,6^+$	$\leq$600	
					16.24	1^+	24	p,n,α_1,γ_0
					16.3	0^-	~250	p,n
					16.35			p_0,α_0
12.35	16.41	(2^+)	60	α_0,p_0	16.43	(2^+)	25 to 100	$p_0,\alpha_1,\alpha_0,n,\gamma$
12.5	16.5		980	p_0,α_0				
					16.71	(2^+)	~25	$\alpha_1,p_0,\alpha_0,n,\gamma$
					16.79	$(2^+)l_p=0$	~70	$p_0,(\alpha_0),\gamma$
12.9	16.8	(4^+)	525	α_0	16.8		~500	α_1,p_0,α_0
13.0	16.9	5^-	900	α_0				
					16.93	(2^+)	~25	n,γ
					17.06	(2^+)	~150	$p,n,\alpha_0,\alpha_1,\gamma$
13.30	17.10	$(1^-,2^+,0^+)$	110	$\alpha_0,(p_0)$	17.13	(2^+)	45	$p,n,(\alpha_1)(\alpha_0),\gamma_0$
					(17.18)	(2^+)	~25	n,γ
					17.29	2^+	84	p,n,α_0,γ_0
					17.31	1^-	~200	$p_0,\alpha_0,\alpha_1(n),(\gamma)$
13.90	17.55	(4^+)	225	α_0	17.5	(2^+)	250	$p,n,\alpha_1,(\gamma)$
13.95	17.60		150	p_0,α_0	17.61	(2^+)	70	$p,n,\alpha_0,(\alpha_1),(\gamma)$
					17.84		~300	$\alpha_0,\alpha_1,(p_0)$
					17.86	(2^+)	105	$p_0,n,\alpha_1,(\alpha_0),\gamma$
					17.97		52	p,n
14.49	18.01	(4^+)	45	α_0	18.05	(2^+)	40	$p_0,n_0,\alpha_0,\alpha_1,\gamma$
					18.13		~220	n,α_0,p_0,α_1
					18.29		100	p_0
14.8	18.23		380	$p_0,(\alpha)_0$	18.3		300	n,α_1,α_0,p
					18.44		~50	α_1,p_0,α_0
15.0	18.4	5^-	680	α_0	18.5		500	$\alpha_0,\alpha_1,(p_0)$
					18.51		~100	p_0
15.2	18.55	$(1^-,5^-)$	190	α_0				
15.46	18.71	(1^-)	75	α_0	(18.70)	(2^+)	~25	n,γ
					18.79		~300	α_1,α_0
15.6	(18.83)		225	p_0,α_0	18.84		~150	p_0,γ
					19.07		$\leq$300	α_1,α_0
15.96	19.10	$(2^+,4^+)$	55	α_0	19.1	(2^+)	~25	n,γ
					19.15	(2^+)	~200	$p_0,\alpha_1,\alpha_0,n,\gamma$
16.13	19.23	(5^-)	30	α_0				
					19.3		~200	p_0,α_0,γ
16.30	19.35	$(4^+,0^+)$	30	α_0				
					19.4		~150	p_0,α_0,α_1
					19.5		~400	$\alpha_0,\alpha_1,p_0,\gamma$
16.73	19.68	even	22	α_0				
17.0	(19.9)	(4^+)	(1100)	α_0				
17.0	19.9	$(2^+,0^+,1^-)$	190	α_0	19.87		~150	p_0,n,α_1,γ
					19.95		~60	p_0,α_1,α_0
					20.1		~250	α_0,n,p_0
					20.2			n,γ
					(20.3)		~1500	p_0,α_0
					(20.33)		~25	n,γ
17.75	(20.44)	(4^+)	150	α_0	20.45		~100	$p_0,(\alpha_1),(\alpha_0)$
					20.59		~300	$\alpha_0,\alpha_1,(p_0),(n),\gamma$
					(20.7)		300 to 800	α_0,α_1
					20.78		~200	p_0,α_1,n,γ
18.4	20.9	7^-	(1000)	α_0				
					20.95		~200	α_1,n,p_0,γ
18.5	21.0	(5^-)	(1200)	α_0				
					21.02		100	p_0
					21.06		~300	α_1,α_0
18.7	(21.2)	(6^+)	(450)	α_0				

TABLE II (*continued*).

This work					Previous work			
E_α (MeV)	E_x (MeV)	J^π	Γ (MeV)	Decay	E_x (MeV)	J^π	Γ (keV)	Decay
					21.25		~200	p_0,n,γ
					21.52		200	p_0,α_1,n,γ
					21.65		~50	$p_0,\alpha_0,(\alpha_1),n,\gamma$
					21.71		50	$p_0,(n),(\gamma)$
					21.92		50	p_0
					22.05		"broad"	d,n

anomalies were made by an examination of the excitation curves measured at angles corresponding to a zero of the Jth Legendre polynomial. If a given resonant structure does not appear at an angle corresponding to a zero of the Jth Legendre polynomial, but is present elsewhere, it is inferred that the resonance has an angular momentum J. Assignments were confirmed by APBM model fits to angular distributions with resonant phase shifts added. A number of unconfirmed spin assignments were made to levels in the compound system. These and other tentative assignments are enclosed in parentheses in Table II.

All calculations were performed with the Florida State University IBM-709 computer.

Optical Model

The optical model cannot reproduce the numerous anomalies in the excitation curves or their effects on the angular distributions. Attempts were made to fit the data with an optical model in order to determine the parameters governing the gross effects. Calculations were carried out with a computer code written by Perey. The optical potential is given by

$$V(r)=U_R\{1+\exp[(r-R_R)/a_R]\}^{-1}+iW_{SI}\{1+\exp[(r-R_I)/a_I]\}^{-1}+4iW_{DI}\exp[(r-R_I)/a_I]\{1+\exp[(r-R_I)/a_I]\}^{-2},$$

where U_R, W_{SI}, and W_{DI} are the real, volume imaginary, and surface imaginary parts of the potential, respectively. The quantities R and a are the radius and diffuseness parameters with subscripts R and I denoting "real" and "imaginary." The nuclear radius parameter r_R used in the computer program is related to R_R and r_{0R} by the equation

$$R_R=r_RA^{1/3}=r_{0R}A^{1/3}+1.3\text{F}.$$

Similarly for R_I, the relation is

$$R_I=r_IA^{1/3}=r_{0I}A^{1/3}+1.3\text{F}.$$

Parameter values used in the fits to the data (Fig. 5) are tabulated in Table III. The quantity σ_R is the optical-model reaction cross section.

Optical-model fits (Fig. 5) to the angular distributions were more satisfactory at forward angles than at back angles. The real potentials of about 100 MeV required to approximately fit angular distributions measured "off resonance" are deeper than the usual 40 to 50 MeV for alpha particles,[8,10] but are not without precedent.[11] Fits to the "on resonance" data measured at 12.1 and 18.0 MeV required even deeper real potentials than those observed "off resonance." In agreement with other work,[10,11] values of the radius parameter r_{0R} in the range 1.4 to 1.6 F yielded the best fits.

Surface imaginary potential values of 3 and 4 MeV were used as seen in Table III. The reaction cross section computed with the optical model and the experimental value are both roughly 500 mb. The geometrically calculated value πR_R^2 is 636 mb for $r_{0R}=1.4$F.

A powerful extension of the optical model is obtained by coupling the target ground state to the low-lying nonspherical excited state(s). The coupled equations approach is discussed in the following paper.[1]

TABLE III. Optical-model parameters for Fig. 5.

Curve	U_R(MeV)	W_{SI}(MeV)	W_{DI}(MeV)	r_R(F)	a_R(F)	r_I(F)	a_I(F)	σ_R(mb)	r_{0R}(F)
A	80	0	4.0	2.07	0.55	2.07	0.3	599	1.5
B	125	0	3.0	1.87	0.5	1.87	0.3	613	1.3
C	150	1.5	0	2.07	0.5	2.07	0.5	558	1.5
D	200	0	4.0	1.97	0.6	1.87	0.3	491	1.4
E	100	0	4.0	1.77	0.6	1.77	0.6	897	1.2
F	110	0	4.0	1.97	0.6	1.97	0.3	647	1.4
G	125	0	1.5	1.97	0.5	1.97	0.5	620	1.4
H	75	0	4.0	1.77	0.6	1.77	0.6	928	1.2
I	110	0	4.0	1.87	0.5	1.87	0.3	483	1.3
J	200	0	4.0	1.97	0.5	1.87	0.3	414	1.4

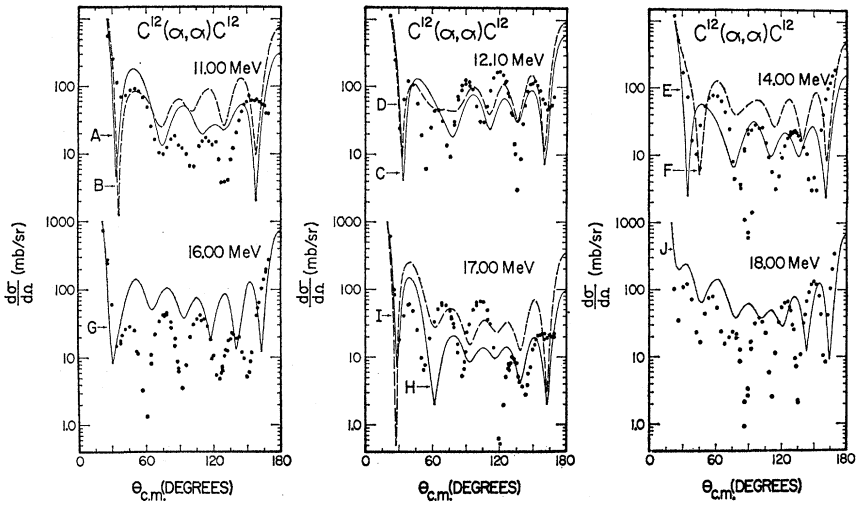

FIG. 5. Optical-model fits to $C^{12}(\alpha,\alpha)C^{12}$ angular distributions. Parameter values are given in Table III.

APB and APBM Models

It is well known that alpha particles are readily absorbed in nuclei.[10] In the Akhiezer-Pomeranchuk model,[12,13] it is assumed that all angular momentum waves with angular momentum l equal to or less than a cutoff angular momentum parameter l_c are totally absorbed. Rather good fits to the elastic scattering data for 22- and 40-MeV alpha particles on medium weight and heavy nuclei have been obtained[10,13,14] using the APB model.

APB model fits to selected angular distributions are shown in Fig. 6. The minima are, of course, too deep, and the back angle cross sections are a little too low. The cutoff angular momentum values do not vary monotonically with energy. This behavior cannot be explained within the framework of the APB model. Fitting parameters and computed results are tabulated in Table IV, where D is the classical distance of closest approach[10] and r_0 is the radius constant. Except at 11 MeV, the values of r_0 are reasonable [r_0 for C^{12} calculated from $D=r_0(12)^{1/3}+1.3\mathrm{F}$]. The classical reaction cross section (calculated from the classical impact parameter) agrees surprisingly well with the experimental value of about 500 mb. The quantum-mechanical reaction cross section

$$\sigma_{RQM}=(\pi/k^2)\sum_l(2l+1)(1-A_l^2)$$

is also tabulated.

Of course, the absorption does not change abruptly with angular momentum l, as is assumed in the APB sharp cutoff approximation. Following McIntyre *et al.*,[15]

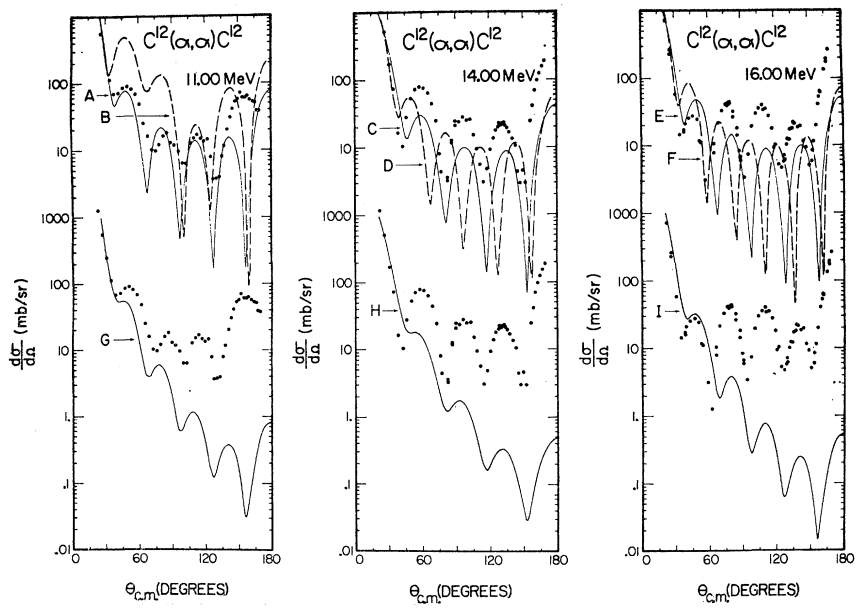

FIG. 6. APB model and APBM model fits to selected angular distributions. Parameters for curves as given in Table IV.

TABLE IV. Parameters for APB model fits and APBM model fits in Fig. 6. The quantity σ_{RQM} is the quantum-mechanical reaction cross section. D, r_0, and σ_{RC} are the classical distance of closest approach, the nuclear radius constant, and reaction cross section, respectively.

Curve	Theoretical curve	$D(F)$	$r_0(F)$	σ_{RQM}	σ_{RC}
A	APB model with cutoff angular momentum l_c, equal to 5.	5.53	1.85	955 mb	594 mb
B	Hypothetical comparison to A with 6 resonant l waves. δ_0 to δ_5 set equal to $\pi/2$.			0	
C	APB model, $l_c=4$.	4.17	1.25	521	330
D	APB model, $l_c=5$.			751	
E	APB model, $l_c=5$.	4.58	1.43	657	450
F	APB model, $l_c=6$.			894	
G	APBM model, $l_c=5.5$, $\Delta l=0.5$			1138	
H	APBM model, $l_c=4.5$, $\Delta l=0.5$			644	
I	APBM model, $l_c=5.5$, $\Delta l=0.5$			782	

the scattering matrix elements are given by a smoothing function

$$A_l=\{1+\exp[(l_c-l)/\Delta l]\}^{-1},$$

where l_C is the cutoff parameter and Δl is an adjustable smoothing parameter. The transition from total absorption of the lower l waves to pure Coulomb scattering of high l waves now takes place gradually. A linear smoothing function was introduced by Ellis and Schecter.[16] A similar dependence of the nuclear phase shift on l was introduced by McIntyre, but will not be utilized here.

If even the very small McIntyre smoothing of $\Delta l=0.5$ is introduced, the elastic cross section at middle and back angles is far too small (Fig. 6, curves G, H, and I). A value of $\Delta l=1.5$ would be more in agreement with typical optical model scattering matrix elements, but would result in even greater disagreement with experiment. Therefore the APBM model with reasonable values of Δl does not fit these data.

APBM Model with Resonances

A phenomenological approach was introduced in which resonance effects were added to the APBM model. Resonant phase shifts were added to the APB model by Bromley[26] and to the optical model by Easlea and Brown.[27]

The mixture of absorption and resonant effects can be readily introduced into the R-matrix formalism. If the differential cross section is given by

$$d\sigma/d\Omega=|f(\theta)|^2,$$

then for a spin-zero projectile and a spin-zero target, Eq. (VII 1.10) in the paper by Lane and Thomas[28] becomes

$$f(\theta)=(2k)^{-1}\{-\eta\csc^2(\theta/2)\exp[-2i\eta\ln\sin(\theta/2)]+i\sum_l(2l+1)(e^{2i\omega_l}-U_l)P_l(\cos\theta)\},$$

where ω_l is the Coulomb phase shift and is given by

$$\omega_l=\sigma_l-\sigma_0=\sum_{m=1}^{l}\tan^{-1}(\eta/m),$$

and $\eta=Z_1Z_2e^2/(\hbar v)$ is the Sommerfeld parameter. The scattering matrix element may be written

$$U_l=e^{2i\omega_l}A_le^{2i\delta_l},$$

where $\delta_l=\beta_l-\phi_l$, $\beta_l=$the resonant phase shift, and $\phi_l=$the "hard-sphere" phase shift. In the Lane and Thomas paper,[28] $\delta_l=\beta_l-\phi_l+\omega_l$.

The APB model may be specified in this expression by the conditions

$$\delta_l=0,\ A_l=0 \text{ for } l\leq l_c, \text{ and } A_l=1 \text{ for } l>l_c,$$

where l_c is the cutoff l value. The APBM model may be specified by

$$A_l=\{1+\exp[(l_c-l)/\Delta l]\}^{-1},$$
$$\delta_l=\Delta\{1+\exp[(l_c-l)/\Delta l]\}^{-1},$$

using McIntyre's notation. Except for a phase factor which does not affect the cross section, these formulas are the same as those obtained by Blair[13] and McIntyre.[15] The McIntyre nuclear phase shift was not used in this work, i.e., $\Delta=0$.

An estimate of the resonant phase shifts may be obtained by using the expression for one channel

$$\delta_l=\tan^{-1}[\Gamma_{\lambda l}/(E-E_{\lambda l})]-\phi_l,$$

where $\Gamma_{\lambda l}$ is the level width and $E_{\lambda l}$ is the resonant energy. The level shift has been neglected in the above. This is a rather crude approximation, but it is expected to give rough estimate of $\Gamma_{\lambda l}$ and $E_{\lambda l}$ from experimental values of δ_l, and it should allow the assignment of a

[26] D. A. Bromley, J. A. Kuehner, and E. Almqvist, Chalk River Report PD-316, 1960 (unpublished).
[27] G. E. Brown (report on work of B. Easlea), *Proceedings of the International Conference on Nuclear Structure*, edited by D. A. Bromley and E. W. Vogt (The University of Toronto Press, Toronto, 1960).
[28] A. M. Lane and R. G. Thomas, Rev. Mod. Phys. **30**, 257 (1958).

TABLE V. Examples of fits in Fig. 7 assuming one resonant phase shift. Curves A and C have no APBM absorption. Curves G and H are examples of quite different APBM parameters, l_c and Δl. σ_R is the reaction cross section.

Curve	l_c	Δl	σ_R	Remarks	
A			0	A_0 to $A_{10}=1.0$; δ_l=zero except	$\delta_6=\pi/2$
B	2.0	1.5	511	APBM formula for A_l; δ_l=zero except	$\delta_6=\pi/2$
C			0	A_0 to $A_{10}=1.0$; δ_l=zero except	$\delta_7=\pi/2$
D	3.8	1.8	725	APBM formula for A_l; δ_l=zero except	$\delta_7=\pi/2$
E	2.2	1.6	461	APBM formula for A_l except $A_4=1.0$; δ_l=zero except	$\delta_4=\pi/2$
F	2.2	1.6	480	APBM formula for A_l except $A_5=1.0$; δ_l=zero except	$\delta_5=\pi/2$
G	2.0	2.0	500	APBM formula for A_l except $A_5=1.0$; δ_l=zero except	$\delta_5=\pi/2$
H	3.0	1.5	508	APBM formula for A_l except $A_5=1.0$; δ_l=zero except	$\delta_5=\pi/2$

spin value to an observed level whose associated phase shift varies much more rapidly than ϕ_l.

Physical significance may be attached to the parameters A_l. Since the outgoing elastic wave is proportional to U_l and therefore to A_l, and since the l-wave reaction cross section is given by $\sigma_{Rl}=(\pi/k^2)(2l+1)(1-U_l^2)=(2k)^{-2}(2l+1)\times(1-A_l^2)$, the value of A_l determines what portion of a particular l wave is absorbed.

Single resonances dominate the $C^{12}(\alpha,\alpha)C^{12}$ angular distributions at bombarding energies of 12.1 and 18.0 MeV (16.2- and 20.7-MeV excitation in O^{16}). Several examples of fits to these are shown in Fig. 7. (See Table V.) With just the single resonance and the Coulomb scattering the fits (curves A and C) are good at the back angles, but deteriorate in the region around 40°. The reaction cross section is zero. Inclusion of the conventional hard sphere phase shifts [29] ϕ_l in addition to the single resonance and Coulomb scattering phase shifts (not shown) makes little improvement in the fits to the elastic scattering data, and none in the reaction cross-section determination. Curves B and D show considerable improvement at the forward angles when the single resonance and the Coulomb scattering are combined with the APBM absorption. Some further change but no improvement over curves B and D was found when the single resonance, Coulomb scattering, APBM absorption, and the hard-sphere phase shifts were all taken into account. The fits at 12.1, 15, and 18 MeV are sufficiently good to assign spins of 6, 5, and 7, respectively, to the dominant resonances. The situation at 13.0 MeV is not as clear. A comparison of curves G and H shows the relative independence of the quality of the fit on the choice of APBM smoothing parameters.

From the experimental excitation curves, it is obvious that many resonances overlap. The inclusion of additional resonant A_l and δ_l in the fits to the angular distributions is therefore reasonable, although the subsequent interpretation becomes more difficult. Additional anomalous phase shifts and A_l's were introduced into the calculations, and the fits to the data are shown in Fig. 8. (See Table VI.)

The effects of the lower l-wave phase shifts are suppressed because of the geometrical $(2l+1)$ factor and because δ_l is unimportant if $A_l\approx 0$. The observed phase shifts of the lower l waves generally change very slowly with energy. In fact the rate of variation with energy of the lower l-wave phase shifts (in this case $l=2$ and 3) is comparable with that of the optical model.

The phase shifts were not extracted for $l=0$ and 1. The less important l waves have an estimated error of about 0.5 to 1.0 rad in δ_l and 0.4 in A_l, and the more important l waves have an estimated error of 0.4 rad in δ_l and 0.2 in A_l. Some of the ambiguity of the extracted phase shifts is exemplified by the fits at 18.00

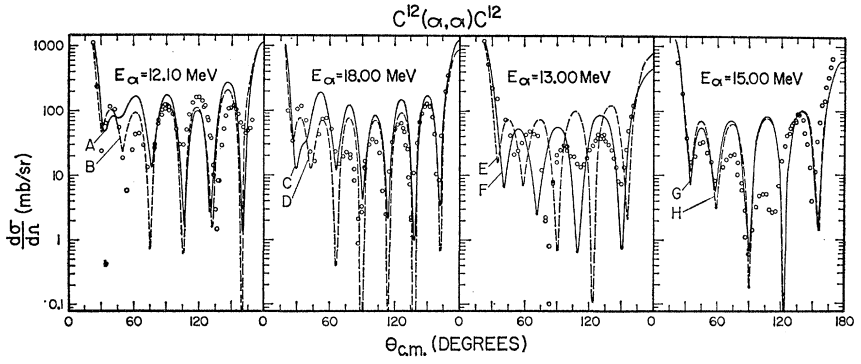

FIG. 7. Fits with one resonant phase shift to angular distribution at prominent resonances. Curves A and C were computed without APBM model absorption and all A_l values are equal to 1.0. In curve A, the value of $\delta_6=\pi/2$ with zero phase shifts for other angular momenta. The resonant phase shift in Curve C is δ_7. Curves B and D include APBM model absorption. Curves E and F at 13 MeV are theoretical fits for $l=4$ and $l=5$, resonances, respectively. At 15 MeV and $l=5$, resonance is assumed and the APBM parameters are varied. Parameters for these curves are shown in Table V.

[29] Calculated at the Chalk River National Laboratory with a computer program written by J. M. Kennedy, communicated by E. Vogt.

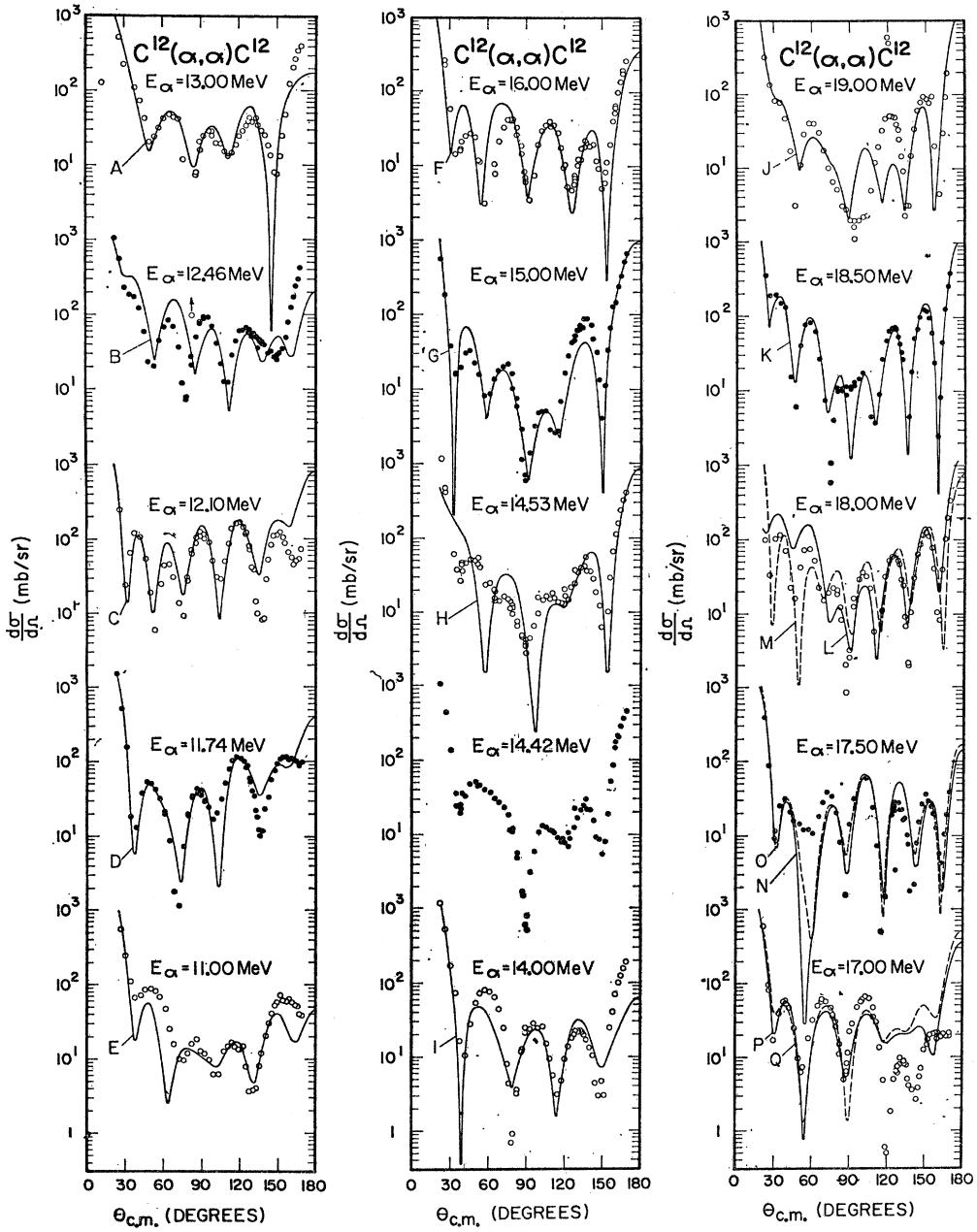

FIG. 8. $C^{12}(\alpha\alpha)C^{12}$ angular distributions and fits with several resonant phase shifts. Parameter values are listed in Table VI.

MeV, where large changes of three of the less important phase shifts do not greatly change the computed results.

Energy Levels and Band Structure in O^{16}

A summary of the previous experimental work on eth energy levels of O^{16} is presented in Table II. The parameters are those of papers abstracted in the Nuclear Data Sheets[30] and some additional references.[1,24,31] Spins assigned to states by gamma-ray induced reactions are enclosed in parentheses where

[30] *Nuclear Data Sheets*, compiled by K. Way *et al.* (National Academy of Sciences, National Council, U. S. Government Printing Office, Washington, D. C.).

[31] R. Weinberg, H. Dieselman, C. Nissim-Sabat, and L. J. Lidofsky, Bull. Am. Phys. Soc. **6**, 26 (1961); J. D. Larson and R. H. Spear, Bull. Am. Phys. Soc. **6**, 505 (1961); J. R. Priest, D. J. Tendam, and E. B. Bleuler, Phys. Rev. **119**, 301 (1960); S. G. Cohen, P. S. Fisher, and E. K. Warburton, Phys. Rev. **121**, 858 (1961); J. Cerny, B. G. Harvey and R. H. Pehl, Nucl. Phys. **29**, 120 (1962); F. W. K. Firk and K. M. Lokan, Phys. Rev. Letters **8**, 321 (1962); G. Dearnaley, D. S. Gemmel, S. W. Hooton, and G. A. Jones, Phys. Letters **1**, 269 (1962); G. Roy, Ph.D. dissertation, Florida State University, 1963 (unpublished); S. Bashkin, R. R. Carlson, and R. A. Douglas, Phys. Rev. **114**, 1543 (1959).

TABLE VI. Parameters for fits in Fig. 8. The equation used is $\frac{d\sigma}{d\Omega}=(2k)^{-2}\left|f(\text{Coulomb})+i\sum_l(2l+1)e^{2i\omega l}(1-A_l e^{2i\delta l})P_l(\cos\theta)\right|^2$.

The dominant resonant phase shifts are printed in boldface type.

Curve	E_α (MeV)	l_c	Δl	σ_R	A_2	δ_2	A_3	δ_3	A_4	δ_4	A_5	δ_5	A_6	δ_6	A_7	δ_7	A_8	δ_8
E	11.00	2.0	1.5	717			0.6	1.8	0.8	0.9	0.6	0.5	0.9	0.4				
D	11.74	2.0	1.6	591	0.6	2.8	0.8	1.8	0.8	2.5	0.7	0.3	0.9	**0.7**				
C	12.1	2.0	1.6	490	0 6	0.2	0.7	2.0	0.8	0.3	0.9	**0.9**	0.95	**1.57**	0.95	0.1		
B	12.46	2.1	1.5	572	0.5	1.57	0.6	1.1	**0.7**	**1.9**	0.8	**2.6**	0.9	**2.6**	1.0	0.2		
A	13.00	2.4	1.6	603	0.5	2.0	0.6	0.8	**0.7**	**1.4**	0.8	2.9	0.9	3.0	0.95	0.1		
I	14.00	2.6	1.6	597	0.5	2.0	0.6	1.7	**0.7**	**1.8**	0.8	0.4	0.9	0.2	0.9	0.2		
H	14.53	2.8	1.6	739			0.5	1.57	0.6	2.9	0.6	**1.4**	0.8	0.1	0.9	0.2		
G	15.00	2.8	1.6	652	0.6	0.7	0.6	2.1	0.6	0.3	0.7	**1.5**	0.8	0.3	0.9	0.2		
F	16.00	2.8	1.8	735	0.5	1.0	0.6	0.6	0.6	0.2	0.7	**1.9**	0.7	0.3	0.8	0.1		
Q	17.00*A*	3.2	1.8	773	0.4	0.9	0.5	1.0	0.5	**1.0**	0.6	**2.1**	0.7	0.1	0.8	0.4		
P	17.00*B*	3.4	1.8	726	0.4	1.3	0.5	1.0	0.5	**0.7**	0.7	**2.3**			0.8	0.5		
O	17.50*A*	3.4	1.8	813	0.4	1.3	0.5	1.6	0.5	**1.6**	0.5	0.2	0.6	0.2	0.8	**0.7**		
N	17.50*B*	3.4	1.8	813	0.4	1.3	0.5	1.8	0.5	**1.8**	0.5	0.2	0.7	0.2	0.8	**0.7**		
M	18.00*A*	3.6	1.8	813	0.4	1.1	0.5	0.7	0.5	**0.8**	0.5	**1.6**	0.6	0.3	0.8	**1.9**	0.9	0.1
L	18.00*B*	3.6	1.8	813	0.4	2.5	0.5	2.8	0.5	**2.6**	0.5	**1.3**	0.6	0.4	0.8	**1.5**	0.9	0.1
K	18.50	3.6	1.8	791	0.4	1.1	0.5	0.7	0.5	**0.8**	0.5	**1.8**	0.6	0.3	0.8	**1.9**	0.9	0.1
J	19.00	3.8	1.8	810	0.4	1.8	0.4	0.2	0.5	**0.9**	0.5	**2.2**	0.5	0.6	0.8	2.6	0.9	0.1

warranted by their tentative nature. Some level widths were estimated from data presented in pertinent references. Decay modes observed in different experiments were assigned to the same level in O^{16} when the level parameters were in agreement. Incomplete information and insufficient precision of the measurements make the groupings tentative in some cases.

For comparison, the level parameters determined in this work are presented. Spin and parity assignments based solely on the qualitative examination of the excitation curves and any questionable assignments from the angular distribution fits are enclosed in parentheses. The excitation energy represents an estimate in that the shapes of the anomalies were not theoretically fitted.

Except for the resonances at 14.6- and 16.2-MeV excitation energy, most of levels which have the largest effects on the angular distributions have not been observed previously. The 6^+ level at 16.2-MeV excitation was observed via the $N^{14}(\alpha,d)O^{16*}$ reaction by Harvey *et al.*[32] Many of the narrow (50 to 200 keV) levels were observed using other reactions, notably $O^{16}(\gamma,p)N^{15}$, $O^{16}(\gamma,n)O^{15}$, $N^{15}(p,\alpha_0)C^{12}$, and $N^{15}(p,\alpha_1)C^{12}$. The tentative spin assignments are not all in agreement with the previous work. Due to the possible error in the spin assignments and the possible existence of two or more levels at approximately the same energy, little can be said about the disagreements. Sufficient information is not available to clarify the disagreement concerning the energy and width of the level near 14.6-MeV excitation energy.

The excitation energies of states with large alpha-particle partial widths show rotational band energy systematics (Fig. 9). One positive parity band and one negative parity band are clearly seen. A second positive parity band is suggested by the dashed line originating at the 0^+ state at excitation energy 11.25 MeV. Other negative parity states may be connected with lines (dashed) with slopes approximately the same as those of the bands. Roth and Wildermuth[20] have assigned cluster configurations to states in O^{16} with angular momentum values up to 4 and excitation energies up to 14 MeV. An extension of this scheme is also shown in Fig. 9.

Many properties of energy levels in light nuclei have been explained in terms of the cluster model of Wildermuth.[33,34] Two different types of rotational bands are described: (1) the accidental type, where the energy separations are largely a result of potential energy differences, and which has a clearly defined cutoff point, and (2), the usual type of rotational band for heavy, deformed nuclei, where the energy difference is largely kinetic energy. If the first positive parity band in O^{16} (starting with the 6.036 MeV 0^+ level) is highly deformed, the 6^+ level at 16.62 MeV would not be the last in that band and an 8^+ level would be expected between 24 and 30 MeV. If the reduced alpha-particle width of the hypothetical 8^+ state is comparable to those of the other band members, the total width would be approximately 400 keV. An extension of the present experiment to higher energies is required to establish the existence or absence of this level. Two bands (not shown in Fig. 9) of a different type may be constructed with the $2f$, $2g$, $2h$, and $2i$; and the $3p$, $3d$, $3f$, $3g$, and $3h$ alpha particle plus C^{12} core cluster states.

A correlation between observed band member

[32] B. G. Harvey, J. Cerny, R. H. Pehl, and E. Rivet, Nucl. Phys. **39**, 160 (1962).

[33] K. Wildermuth and T. Kannellopoulos, CERN Report 59-23, 1959 (unpublished); R. K. Sheline and K. Wildermuth, Nucl. Phys. **21**, 196 (1961).

[34] K. Wildermuth and Th. Kanellopoulos, Nucl. Phys. **9**, 449 (1958/59).

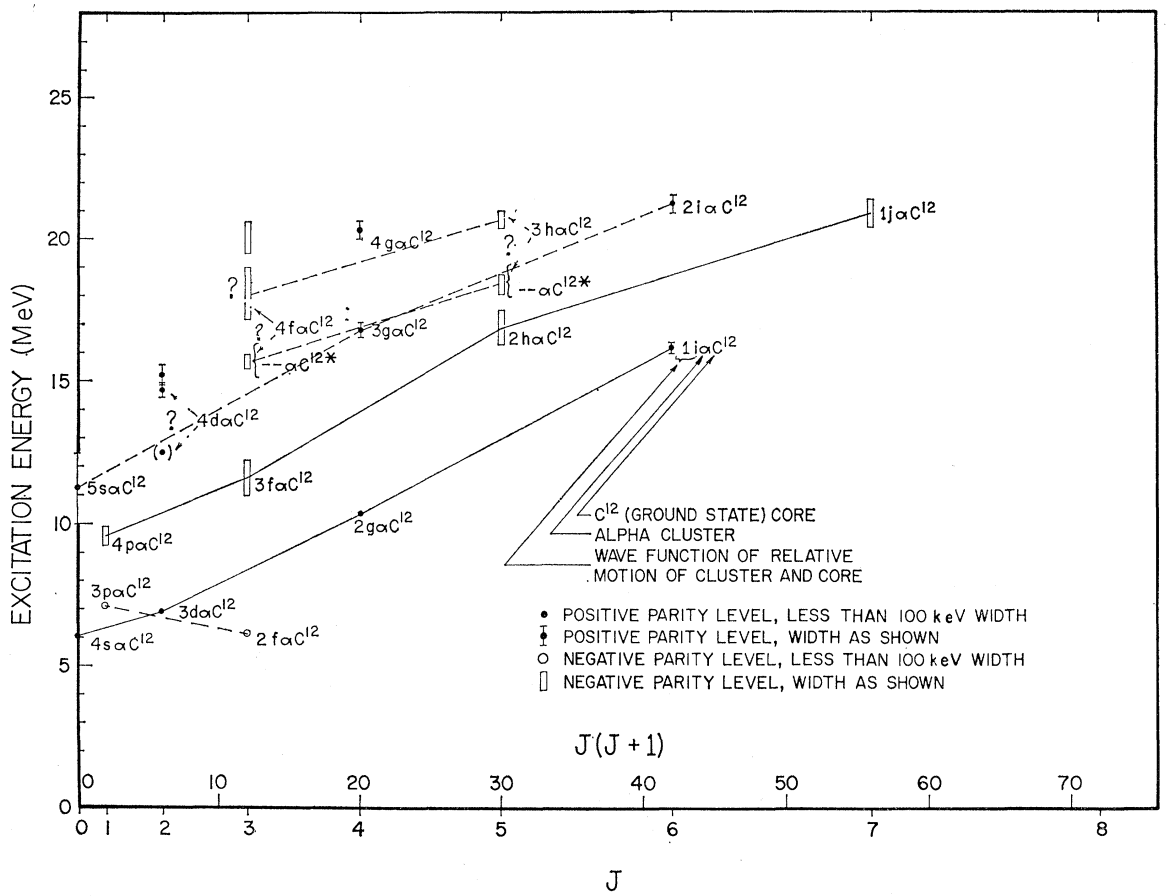

FIG. 9. Cluster states and rotational bands in O^{16}. A number of narrow levels of spin 0, 1, 2, 3, and 4 have been omitted for clarity.

widths and the rotational energy parameter is discussed in a separate paper.[35]

Harvey *et al.*[32] describe the last four nucleons of the 16.2-MeV state in O^{16} with a $(p_{1/2})_1^2\ (d_{5/2})_5^2$ shell-model wave function. The properties of this shell-model configuration such as the nucleon motion and the number of oscillator quanta are similar to those of the cluster-model wave-function assignment $1h\alpha C^{12}$.

V. SUMMARY

The carbon plus alpha-particle entrance channel biased the results of this study of O^{16}. The possible spins and parities of the compound system are restricted, and the formation of alpha-particle cluster states is enhanced. Nevertheless, a large number of resonances appear in the excitation curves.

Fits to the data with the optical model were not good and required an anomalous variation of the parameters with energy. Real well depths in excess of 100 MeV were necessary to fit the data. This is approximately four times the nucleon well depth less the binding energy.

A sharp cutoff (APB) model analysis is suggested by the small alpha-particle mean free path in nuclear matter. This model contains no mechanism which will reproduce the frequent anomalies, but surprisingly good fits were obtained with the APB model for 3 of the 15 angular distributions.

Satisfactory fits to the data were obtained with a smooth cutoff (APBM) model by substituting resonant phase shifts where appropriate. This model of nuclear scattering provides a convenient first approximation to a detailed set of phase shifts. Spins and parities of the prominent levels in O^{16} were obtained from the fits to the angular distributions.

Two bands of levels in O^{16} which obey rotational band energy systematics were observed. Most of the member levels have large alpha-particle widths. Additional bands are tentatively indicated by the data.

ACKNOWLEDGMENTS

The authors wish to thank Dr. W. E. Hunt, Dr. M. K. Mehta, J. D. Marshall, and J. B. Seaborn for assistance in performing the experiment. The APBM smooth cutoff computer program of J. Alster[36] was modified by S. Sterk. Dr. F. G. Perey of the Oak Ridge National Laboratory kindly provided the authors with a copy of his optical-model computer program.

[35] R. H. Davis, Bull. Am. Phys. Soc. 8, 25 (1963).

[36] J. Alster, University of California Radiation Laboratory Report UCRL-9650, 1961 (unpublished).